2004-10-18

Integrated optical waveguides with liquid cores

Aaron R. Hawkins
hawkins@ee.byu.edu

John P. Barber
johnpbarber@yahoo.com

Dongliang Yin

D. W. Deamer

Holger Schmidt

Original Publication Citation

Yin, D., D. W. Deamer, H. Schmidt, J. P. Barber, and A. R. Hawkins. "Integrated optical waveguides with liquid cores." Applied Physics Letters 85 (24): 3477-3479

Integrated optical waveguides with liquid cores

D. Yin, D. W. Deamer, and H. Schmidt[a)]
School of Engineering, University of California, Santa Cruz, 1156 High Street, Santa Cruz, California 95064

J. P. Barber and A. R. Hawkins
ECE Department, Brigham Young University, 459 Clyde Building, Provo, Utah 84602

(Received 23 December 2003; accepted 20 August 2004)

We report the design, fabrication, and demonstration of single-mode integrated optical waveguides with liquid cores. The principle of the device is based on antiresonant reflecting optical (ARROW) waveguides with hollow cores. We describe design principles for waveguide loss optimization down to 0.1/cm. Using a fabrication process based on conventional silicon microfabrication and sacrificial core layers, waveguides of varying widths and lengths with volumes covering the pico- to nanoliter range were fabricated. We observe confined mode propagation, measure waveguide losses of 2.4/cm, and demonstrate that the waveguides possess tailorable wavelength selectivity. The potential for highly integrated, sensitive devices based on these properties of the ARROW waveguides is discussed. © *2004 American Institute of Physics*. [DOI: 10.1063/1.1807966]

Numerous applications could benefit from the availability of an integrated optical platform that enables light propagation through small volumes of liquids on a chip. Such applications include chemical sensing, fluorescence spectroscopy in biology, biochemistry, biomedicine, flow cytometry, pollution monitoring, and others. Generally, optical sensing and spectroscopy of liquids has been carried out in channels with cores wider than 50 μm, typically using glass or Pyrex channels with associated optical coupling losses when connected to optical fibers.[1,2] For studies with extremely high sensitivity such as single-molecule detection in molecular biology, bulky three-dimensional microscopy setups are being used.[3,4] In contrast, the features and advantages of an integrated approach are compact size, planar geometry, potential for massively parallel architectures with multiple waveguides on one chip, increased sensitivity, and higher level integration with additional sources or detection elements. However, it is generally not possible to create single-mode integrated optical waveguides with liquid or hollow cores using conventional waveguides that are based on index guiding. Such nonsolid core materials have lower refractive indices (approximately 1.33 for water, 1 for air) than typical solid materials used for integrated optics, thus precluding confined light propagation over appreciable distances in small (micron-sized) cores. Currently, the only cladding materials suitable for index guiding of light in an aqueous core are amorphous copolymers of polytetrafluoroethylene (Teflon AF) with an index of $\geqslant 1.29$.[5] However, waveguides with Teflon AF coatings have large diameters ($\geqslant 50$ μm) and are not compatible with conventional microfabrication processes in integrated optics. Possible alternative ways to guide light in low-index media include photonic crystal structures such as holey fibers and omniguides.[6,7] These can also not easily be integrated in two-dimensional planar structures and rely on long-range periodicity to open up the required photonic bandgaps.

We have proposed an approach to achieve all of the above desired attributes that enables single-mode light propagation in liquids on a chip.[8] The concept is based on antiresonant reflecting optical (ARROW) waveguides.[9] The ARROW principle is depicted in Fig. 1(a). The low-index core is surrounded by high-index cladding layers with a thickness chosen such that they act as a highly reflective Fabry–Perot cavity for the transverse wave vector k_T at the design wavelength. The confinement that is created in this way allows for low-loss propagation over large distances (many centimeters) despite the fact that the optical mode is

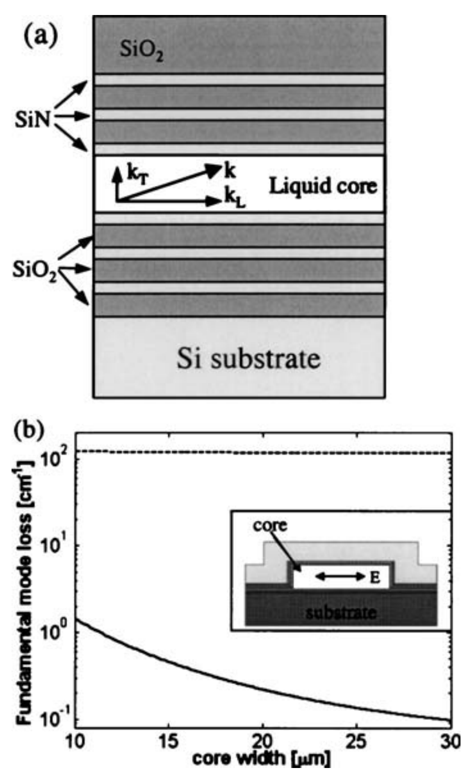

FIG. 1. (a) Side view of ARROW waveguide structure with liquid core. High-index cladding layers act as Fabry–Perot reflectors for the transverse wave vector k_T. (b) Waveguide loss for fundamental ARROW mode vs core width (solid line) and nonguiding water/glass capillary (dashed line) ($d_c = 3.5$ μm). Inset: Front view of ARROW structure with incident polarization.

[a)]Electronic mail: hschmidt@soe.ucsc.edu

leaky. The concept has been utilized mainly for semiconductor laser applications[10,11] using ARROW confinement either in transverse or lateral direction. A method to fabricate hollow waveguides based on the ARROW principle was proposed in which MEMS technology and wafer bonding would be combined.[12] Here, we present the design, fabrication, and optical characterization of integrated ARROW structures with liquid cores using conventional silicon microfabrication and sacrificial core layers. We demonstrate optical confinement and propagation through micron-scale fluid channels that contain picoliter to nanoliter volumes and present measurements of the waveguide loss at various wavelengths. In addition, we investigate the wavelength selectivity of the structures and how the wavelength response can be tailored by adjusting the cladding layer thickness.

For sample and process design, we chose silicon nitride (n=2.05) and silicon dioxide (n=1.46) as ARROW cladding materials due to their compatibility with silicon microfabrication and the potential for further integration. The most important design consideration is the minimization of waveguide loss. The minimum required thickness d_i for the ith cladding layer away from the core can be calculated in the same way as for a solid-core ARROW and is given by[13]

$$d_i = \frac{\lambda}{4\sqrt{(n_i^2 - n_c^2) + \frac{\lambda^2}{4d_c^2}}}, \tag{1}$$

for cores with $d_c = \lambda$, where n_i and n_c are the cladding and core refractive indices, d_c is the core thickness, and λ is the wavelength. Following Eq. (1), a sample for low-loss propagation in water (n=1.33) can be designed. As will be shown in the following, these ARROW waveguides can be built with rectangular cores surrounded by the dielectric cladding layers as shown in the inset of Fig. 1(b) along with the polarization direction of the incident light. The resulting wave guide loss can be calculated either by using a three-dimensional mode solver [FIMMWAVE, (c) Photon Design] or to a very good approximation by adding the one-dimensional losses for a TE mode in transverse and a TM mode in lateral direction. Figure 1(b) shows the loss as a function of core width for a sample with d_c=3.5 μm, d_1=110 nm, d_2=281 nm, and λ=690 nm (solid line). The loss is two to three orders of magnitude lower than in a channel clad by SiO_2 only (dashed line). It decreases with increasing core width and is dominated by the loss in the lateral direction. A rectangular core with three top and bottom cladding periods represents a compromise between achieving low loss and fabrication complexity. Additional cladding layers would further reduce the loss, but in reality other loss mechanisms such as scattering will eventually dominate. The rectangular shape is easy to realize but leads to relatively high lateral loss. Other lateral confinement methods such as a ridge in the top SiO_2 layer or lateral variation of the core thickness add some complexity to the fabrication process but can lead to further improvement.

Two major criteria were addressed for successful waveguide fabrication: choosing a sacrificial core material that leads to smooth sidewalls and can be etched with high selectivity and, second, growth of a thick SiO_2 top layer which provides mechanical stability as well as another antiresonant confinement layer. Based on these principles, we developed the following fabrication process: (1) Alternating oxide and nitride layers for the bottom reflector were deposited on a silicon substrate using plasma-enhanced vapor deposition at temperatures between 250 and 300 °C. (2) Subsequently, a 3.5-μm-thick sacrificial layer of photosensitive polyimide (SU-8) was deposited and patterned into 2-cm-long ridges of varying width (6–50 μm). (3) The top ARROW layers and the SiO_2 cap layer were deposited. (4) To create the channel for the fluid, the SU-8 layer was removed using a solution of H_2O_2 and H_2SO_4 at 85 °C providing the necessary directional etch selectivity. A SEM image of a completed device with a 3.5 by 12 μm core is shown in Fig. 2, demonstrating almost perfectly rectangular hollow cores with excellent smoothness.

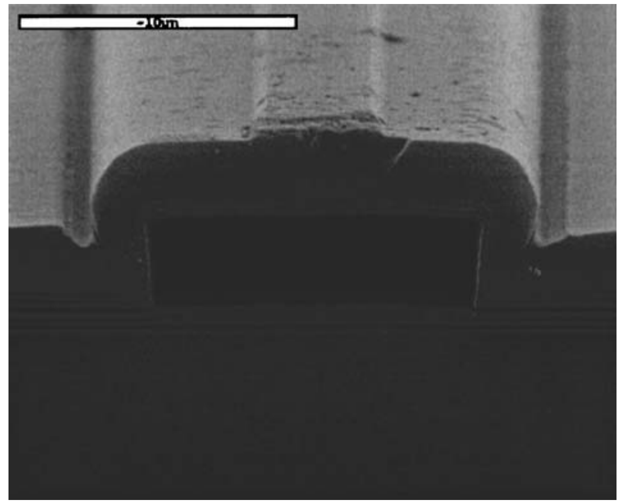

FIG. 2. SEM image of hollow-core ARROW waveguide (core dimensions: 3.5 by 12 μm).

For optical characterization, we studied samples whose layers were optimized for propagation in air (d_1=109 nm, d_2=184 nm), but which also exhibit low loss when filled with liquids. They were cleaved into waveguides with variable length (0.5–8 mm) and light from a He–Ne laser at 633 nm or a diode laser at 785 nm with up to 1 mW power was coupled into the waveguide cores using single-mode fiber. For measurements with liquid cores, the cores were filled with ethylene glycol and then mounted on a translation stage for transmission measurements. Ethylene glycol (n=1.43) was used because it evaporates more slowly than water allowing for longer measurement times. The near-field image of the mode profile at the output facet was recorded using magnifying optics (0.85 NA lens, 60:1 magnification) and a CCD camera (BeamPro Model 2320, Photon Inc). The image of the output facet is shown in Fig. 3(a) for the same core dimensions as in Fig. 2, corresponding to a liquid volume of 21 pl inside the waveguide. The black lines outline the core and the top of the waveguide for clarity. The optical mode is clearly confined inside the liquid core. The facet is simultaneously illuminated with a lamp to identify the core area during alignment, resulting also in a bright strip of reflected light from the lamp below the core. The mode intensity profile with the illumination turned off is shown in the inset. The fundamental ARROW mode is clearly dominant as higher order modes possess significantly higher loss and are not detected at the output facet. Figure 3(b) shows transverse (squares) and lateral (circles) cross sections through the center of the waveguide in comparison with the theoretically

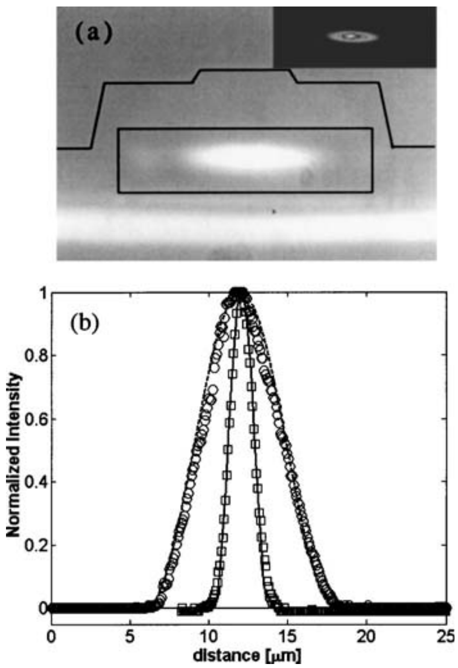

FIG. 3. (a) Output facet image of mode propagating in liquid core ARROW waveguide. Black lines: Outline of sample for clarity. Inset: Intensity mode profile (near-field). (b) Comparison of observed transverse (squares) and lateral (circles) mode profiles in waveguide center with theoretical prediction (lines).

expected profile (lines) assuming ARROW confinement in both transverse and lateral direction. Excellent agreement is observed without using any fitting parameters and a mode area (full width at half maximum) of 7.8 μm^2 is measured. This also indicates that the ridge did not have the correct height to affect the lateral confinement for this sample.

Next, the waveguide loss was determined by recording the intensity throughput as a function of waveguide length. The results for a sample with core width 24 μm are shown in Fig. 4(a). By fitting the data to a decaying exponential, a loss of 2.4 cm^{-1} is observed at 633 nm. At 785 nm, we could not observe any transmission which implies a loss of at least 10 cm^{-1} based on the current sensitivity of our setup. Both loss data are shown in Fig. 4(b) along with the calculated loss values (1.14 and 11.7 cm^{-1}, respectively) including both contributions from higher order modes and the slightly smaller thickness of the laterally confining ARROW layers. The experimental values are in good qualitative agreement with calculations. The discrepancy is mainly due to scattering and absorption losses in the waveguide and thickness variations within the ARROW confinement layers. We emphasize that the wavelength dependence of the loss is strong and can be tailored by choosing the ARROW layer thicknesses while maintaining low loss at one design wavelength. This wavelength selectivity is demonstrated by the dashed line in Fig. 4(b), showing the fundamental mode loss of an optimized structure with high loss of 81 cm^{-1} at 633 nm, but low loss of 0.15 cm^{-1} at 690 nm (arrows in Fig. 4). These wavelengths lie within the absorption and emission bands of conventional dyes (e.g., Alexa 647), which makes these waveguides especially attractive for fluorescence and Raman scattering studies of biomolecules.

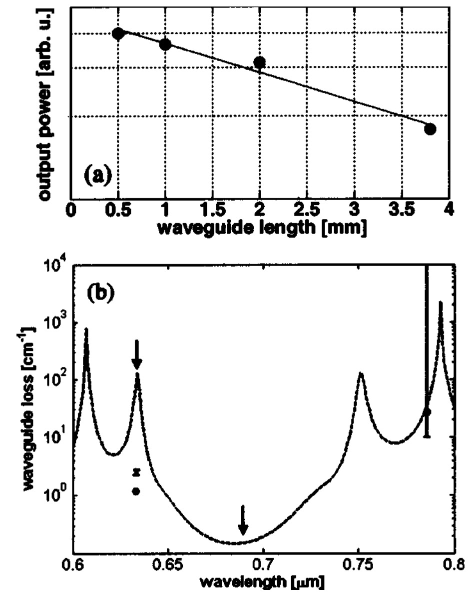

FIG. 4. (a) Circles: Transmitted intensity vs waveguide length (λ =633 nm). Line: Exponential fit. (b) Waveguide loss vs wavelength. Bars: Experimental values (ethylene glycol core); circles: calculation (ethylene glycol core), dashed line: optimized design (water core) for propagation at 690 nm and rejection at 633 nm (arrows).

In summary, we have demonstrated low-loss light propagation in liquid channels integrated on a semiconductor chip by fabricating and testing integrated ARROW waveguides with liquid cores. These devices can be used to guide light through picoliter to nanoliter volumes. In addition to their small size, they offer properties that are desirable for many applications, especially sensing in liquids and studies of single biomolecules. These include single-mode propagation, potential for integration of numerous waveguides, and tailorable wavelength selectivity.

The authors would like to thank E. Despain for assistance with SEM imaging. This work is supported by the NIBIB/NIH.

[1]D. Ivnitski, I. Abdel-Hamid, P. Atanasov, and E. Wilkins, Biosens. Bioelectron. **14**, 599 (1999).
[2]M. Curcio, P. Stalhandske, P. Lindberg, and J. Roeraade, Electrophoresis **23**, 1467 (2002).
[3]M. J. Levene, J. Korlach, S. Turner, M. Fouquet, H. Craighead, and W. W. Webb, Science **299**, 682 (2003).
[4]M. Medina, and P. Schwille, BioEssays **24**, 758 (2002).
[5]J. H. Lowry, J. S. Mendelowitz, and N. S. Subramanian, Opt. Eng. **31**, 1982 (1992).
[6]P. Russell, Laser Focus World **38**, 77 (2002).
[7]Y. Fink, J. N. Winn, S. Fan, C. Chen, J. Michel, J. D. Joannopoulos, and E. L. Thomas, Science **282**, 1679 (1998).
[8]H. Schmidt, D. Yin, and A. R. Hawkins, Proceedings of the Integrated Optics Research Conference, Washington, DC, 2003.
[9]M. A. Duguay, Y. Kokubun, T. Koch, and L. Pfeiffer, Appl. Phys. Lett. **49**, 13 (1986).
[10]L. J. Mawst, D. Botez, C. Zmudzinski, and C. Tu, IEEE Photonics Technol. Lett. **4**, 1204 (1992).
[11]S. G. Patterson, G. S. Petrich, R. J. Ram, and L. A. Kolodiejski, Electron. Lett. **35**, 395 (1999).
[12]R. Bernini, S. Campopiano, and L. Zeni, IEEE J. Sel. Top. Quantum Electron. **8**, 106 (2002).
[13]J-L. Archambault, R. J. Black, S. Lacroix, and J. Bures, J. Lightwave Technol. **11**, 416 (1993).